ARTHRITIS & RHEUMATOLOGY
Vol. 68, No. 2, February 2016, pp 359–369
DOI 10.1002/art.39442

Receptor Protein Tyrosine Phosphatase α–Mediated Enhancement of Rheumatoid Synovial Fibroblast Signaling and Promotion of Arthritis in Mice

Stephanie M. Stanford,[1] Mattias N. D. Svensson,[1] Cristiano Sacchetti,[1] Caila A. Pilo,[1] Dennis J. Wu,[1] William B. Kiosses,[2] Annelie Hellvard,[3] Brith Bergum,[3] German R. Aleman Muench,[1] Christian Elly,[1] Yun-Cai Liu,[1] Jeroen den Hertog,[4] Ari Elson,[5] Jan Sap,[6] Piotr Mydel,[3] David L. Boyle,[7] Maripat Corr,[7] Gary S. Firestein,[7] and Nunzio Bottini[1]

Objective. **During rheumatoid arthritis (RA), fibroblast-like synoviocytes (FLS) critically promote disease pathogenesis by aggressively invading the extracellular matrix of the joint. The focal adhesion kinase (FAK) signaling pathway is emerging as a contributor to the anomalous behavior of RA FLS. The receptor protein tyrosine phosphatase α (RPTPα), which is encoded by the *PTPRA* gene, is a key promoter of FAK signaling. The aim of this study was to investigate whether RPTPα mediates FLS aggressiveness and RA pathogenesis.**

Methods. **Through RPTPα knockdown, we assessed FLS gene expression by quantitative polymerase chain reaction analysis and enzyme-linked immunosorbent assay, invasion and migration by Transwell assays, survival by annexin V and propidium iodide staining, adhesion and spreading by immunofluorescence microscopy, and activation of signaling pathways by Western blotting of FLS lysates. Arthritis development was examined in RPTPα-knockout (KO) mice using the K/BxN serum–transfer model. The contribution of radiosensitive and radioresistant cells to disease was evaluated by reciprocal bone marrow transplantation.**

Results. **RPTPα was enriched in the RA synovial lining. RPTPα knockdown impaired RA FLS survival, spreading, migration, invasiveness, and responsiveness to platelet-derived growth factor, tumor necrosis factor, and interleukin-1 stimulation. These phenotypes correlated with increased phosphorylation of Src on inhibitory Y^{527} and decreased phosphorylation of FAK on stimulatory Y^{397}. Treatment of RA FLS with an inhibitor of FAK phenocopied the knockdown of RPTPα. RPTPα-KO mice were protected from arthritis development, which was due to radioresistant cells.**

Conclusion. **By regulating the phosphorylation of Src and FAK, RPTPα mediates proinflammatory and proinvasive signaling in RA FLS, correlating with the promotion of disease in an FLS-dependent model of RA.**

Fibroblast-like synoviocytes (FLS) control the composition of the synovial fluid and extracellular matrix (ECM) of the joint lining. In rheumatoid arthritis (RA), FLS become aggressive and invasive, contributing to disease pathology. FLS produce matrix metalloproteinases (MMPs) that break down the ECM, directly invade and digest the articular cartilage, promote bone erosion, and promote inflammation through secretion of interleukin-6

Publication 1847 from the La Jolla Institute for Allergy and Immunology.

Supported by the NIH (grants AR-47825 and AI-070555 to Dr. Firestein, grant AR-066053 to Dr. Bottini, and Clinical and Translational Science Award UL1-TR-000100 to the University of California at San Diego), the Arthritis National Research Foundation (grant to Dr. Stanford), and the La Jolla Institute for Allergy and Immunology (institutional funding to Dr. Bottini).

[1]Stephanie M. Stanford, PhD, Mattias N. D. Svensson, PhD, Cristiano Sacchetti, PhD, Caila A. Pilo, BS, Dennis J. Wu, BS, German R. Aleman Muench, PhD, Christian Elly, BS, Yun-Cai Liu, PhD, Nunzio Bottini, MD, PhD: La Jolla Institute for Allergy and Immunology, La Jolla, California; [2]William B. Kiosses, PhD: The Scripps Research Institute, La Jolla, California; [3]Annelie Hellvard, PhD, Brith Bergum, MSc, Piotr Mydel, MD, PhD: Broegelmann Research Laboratory and University of Bergen, Bergen, Norway; [4]Jeroen den Hertog, PhD: Hubrecht Institute-Koninklijke Nederlands Akademie van Wetenschappen and University Medical Center Utrecht, Utrecht, The Netherlands, and Institute of Biology, Leiden, The Netherlands; [5]Ari Elson, PhD: Weizmann Institute of Science, Rehovot, Israel; [6]Jan Sap, PhD: Université Paris Diderot, Sorbonne Paris Cité, Paris, France; [7]David L. Boyle, BS, Maripat Corr, MD, Gary S. Firestein, MD: University of California at San Diego School of Medicine, La Jolla.

Address correspondence to Nunzio Bottini, MD, PhD, Division of Cellular Biology, La Jolla Institute for Allergy and Immunology, 9420 Athena Circle, La Jolla, CA 92037. E-mail: nunzio@liai.org.

Submitted for publication November 27, 2014; accepted in revised form September 15, 2015.

(IL-6), chemokines, and other mediators of inflammation (1–4). FLS are highly sensitive to the inflammatory environment present in rheumatoid joints. Growth factors, especially platelet-derived growth factor (PDGF), stimulate FLS invasiveness. Inflammatory cytokines, in particular, tumor necrosis factor (TNF) and interleukin-1β (IL-1β), enhance FLS aggressiveness, proinflammatory features, and MMP production (4). Targeting of molecules that control FLS invasiveness and inflammatory output is considered an option for development of new therapies for RA (4–6).

Many signaling pathways that control FLS behavior rely upon tyrosine phosphorylation of proteins (4), which results from the balanced action of protein tyrosine kinases (PTKs) and protein tyrosine phosphatases (PTPs). The focal adhesion kinase (FAK) pathway is emerging as an important mediator of the anomalous behavior of RA FLS. FAK is a ubiquitously expressed nonreceptor tyrosine kinase that acts as a critical mediator of cell motility and invasiveness (7) and promotes cell survival (8). FAK activation is dependent upon tyrosine-397 (Y^{397}) phosphorylation induced by integrin-mediated cell adhesion (7,8). This site can be either autophosphorylated by FAK or phosphorylated by Src family kinases (SFKs), which use phospho-Y^{397} as a docking site by which to activate FAK through phosphorylation of other tyrosine residues. Increased phospho-FAK levels have been shown in synovial lining cells from RA tissue as compared to normal tissue (9), and a recent epigenomics study showed that the FAK pathway is a hotspot of epigenetic anomalies in RA FLS (10). These findings suggest that anomalous FAK activation may play a significant role in RA FLS aggressiveness.

We recently reported that the PTP SH2 domain–containing phosphatase 2 (SHP-2), which is overexpressed in RA FLS versus osteoarthritis FLS, mediates the aggressive RA FLS phenotype by promoting FAK activation, leading to enhanced FLS survival, invasiveness, and responsiveness to PDGF and TNF stimulation (11). We noted that receptor PTPα (RPTPα), another PTP that regulates FAK activity in fibroblast and solid cancer cell lines (12–14), was also highly expressed in RA FLS (11).

RPTPα, which is encoded by the *PTPRA* gene, is ubiquitously expressed (15,16). It is a critical positive regulator of signaling through dephosphorylation of the SFK C-terminal inhibitory tyrosine residue (Y^{527} in Src) (13,14,16–18). Dephosphorylation of Src-Y^{527} enhances Src activation, leading to tyrosine phosphorylation of FAK-Y^{397} and other substrates. Embryonic fibroblasts from RPTPα-knockout (KO) mice showed increased Src-Y^{527} phosphorylation, reduced SFK activity, reduced FAK-Y^{397} phosphorylation, and reduced Src/FAK association (12,14,19). RPTPα-KO mice were recently reported to be protected from experimentally induced lung fibrosis, a phenotype mediated by reduced profibrotic transforming growth factor β (TGFβ) signaling in lung fibroblasts from RPTPα-KO mice (20). These findings, together with the role of RPTPα in Src and FAK regulation as well as the hypothesized role of the FAK pathway in the pathogenic behavior of RA FLS, led us to investigate a potential role of RPTPα in RA FLS pathophysiology.

We demonstrate herein that RPTPα regulates the phosphorylation of Src and FAK in RA FLS and promotes RA FLS aggressiveness by mediating signaling in response to TNF, IL-1β, and PDGF. We also report that RPTPα-KO mice are protected from arthritis in an FLS-dependent model of disease, which supports a model whereby promotion of the FAK pathway by RPTPα in FLS contributes to the pathogenesis of RA.

MATERIALS AND METHODS

Antibodies and other reagents. The rabbit anti-RPTPα antibody has been described previously (14). Other primary antibodies were purchased from Cell Signaling Technology and secondary antibodies from GE Healthcare Life Sciences. TNFα, IL-1β, and PDGF-BB were purchased from eBioscience. The FAK inhibitor PF573228 was purchased from EMD Millipore. The Akt inhibitor MK2206 was purchased from SelleckChem. Except where indicated otherwise, the other reagents were purchased from Sigma-Aldrich.

Immunohistochemical (IHC) analysis of synovial tissue. The anti-RPTPα antibody was optimized for IHC analysis using sections of arthritic ankles from wild-type (WT) and RPTPα-KO mice (data not shown). Paraffin-embedded sections of human RA synovial tissue were obtained from the Clinical and Translational Research Institute (CTRI) Biorepository at the University of California, San Diego (UCSD). Slides were deparaffinized, rehydrated, pretreated for 10 minutes with boiling citrate antigen-retrieval buffer (1.9 m*M* citric acid, 10 m*M* Tris–sodium citrate, pH 6.0), and treated for 10 minutes with 3% H_2O_2. Slides were blocked with 5% goat serum for 1 hour at room temperature and then incubated overnight at 4°C with rabbit anti-RPTPα antibody or control rabbit IgG (1:100 dilution in 5% bovine serum albumin [BSA]). Slides were washed and incubated for 30 minutes with SignalStain Boost IHC detection reagent (horseradish peroxidase–labeled, rabbit; Cell Signaling Technologies), then incubated for 5 minutes with 3,3′-diaminobenzidine substrate (Sigma-Aldrich), and counterstained with hematoxylin. Slide images were obtained using a Nikon Eclipse 80i microscope.

Preparation of FLS. FLS were obtained from the CTRI Biorepository at UCSD. Each line was previously derived from discarded synovial tissue from different RA patients undergoing synovectomy, as previously described (21). The diagnosis of RA conformed to the American College of Rheumatology 1987 revised criteria (22). FLS were cultured in Dulbecco's modified Eagle's medium (DMEM; Mediatech) with 10% fetal bovine serum (FBS; Omega Scientific), 2 m*M* L-glutamine, 50 μg/ml gentamicin, 100 units/ml penicillin, and 100 μg/ml streptomycin (Life Technologies) at 37°C in a humidified atmosphere containing 5% CO_2. For all experiments, FLS were used between pas-

sages 4 and 10, and the cells were synchronized in 0.1% FBS (serum-starvation medium) for 48 hours prior to analysis or functional assays.

Quantitative polymerase chain reaction (qPCR). RNA was extracted using RNeasy kits (Qiagen) or TRIzol reagent (Life Technologies). For lysis of FLS, adherent cells were first washed in phosphate buffered saline (PBS) and then lysed in the culture plate. Complementary DNA was synthesized using SuperScript III First-Strand Synthesis SuperMix (Life Technologies). Then, qPCR was performed using a Roche LightCycler 480 analyzer, with primer assays from SABiosciences/Qiagen. Reactions were measured in triplicate, and data were normalized to the expression levels of the housekeeping gene GAPDH or RNA polymerase II (23).

FLS treatment with cell-permeable antisense oligonucleotide (PMO). FLS were treated for 7 days with 2.5 μM PMO (Gene Tools). PMO was replaced in fresh culture medium after 3 days and in serum-starvation medium after 5 days.

Enzyme-linked immunosorbent assays (ELISAs). Levels of secreted human IL-6 and CXCL10 were measured using ELISAs obtained from BioLegend.

Transwell invasion and migration assays. In vitro invasion assays were performed in Transwell systems as previously described (24,25). Following treatment with PMO, equal numbers of live RA FLS were resuspended in assay medium (DMEM with 0.5% BSA) and allowed to invade through BD BioCoat GFR Matrigel chambers in response to treatment with 50 ng/ml of PDGF-BB for 48 hours. Cells were prestained with 2 μM CellTracker Green or were stained postinvasion with 2 μM Hoechst 33242 (Life Technologies) for 30 minutes at room temperature. Fluorescence of invading cells on each membrane was visualized using a Nikon Eclipse 80i microscope. Images were acquired from 4 nonoverlapping fields per membrane, and the numbers of invading cells in each field were counted using ImageJ software (National Institutes of Health). Each experiment included 3–4 membranes per sample.

Transwell migration assays were similarly performed. Following treatment with PMO, equal numbers of live RA FLS were allowed to migrate through uncoated Transwell chambers in response to treatment with 5% FBS for 24 hours. Each experiment included 3–4 membranes per sample.

Survival and apoptosis assay. Following treatment with PMO, RA FLS were washed and incubated for an additional 24 hours in serum-starvation medium. Adherent and nonadherent cells were collected and stained with Alexa Fluor 647–conjugated annexin V and propidium iodide (PI) according to the manufacturer's instructions (BioLegend). Cell fluorescence was assessed by fluorescence-activated cell sorting (FACS) using a BD LSRII FACS (BD Biosciences), and counts and percentages of live (annexin V–/PI–), early apoptotic (annexin V+/PI–), or late apoptotic/necrotic (annexin V+/PI+) cells were obtained. The data were analyzed for statistical significance using the chi-square test for independence.

Spreading and adhesion assay. Following treatment with PMO, equal numbers of live RA FLS were resuspended in FLS medium containing 5% FBS and allowed to adhere to coverslips that had been coated with 20 μg/ml of fibronectin at 37°C for 15, 30, or 60 minutes. Cells were then fixed in 4% paraformaldehyde for 5 minutes, permeabilized in 0.2% Triton X-100 for 2 minutes, and stained with 5 units/ml of Alexa Fluor 568–conjugated phalloidin and 2 μg/ml of Hoechst 33242 for 20 minutes (Life Technologies). Samples were imaged with an Olympus FV10i confocal laser scanning microscope. Using FV10i acquisition software, each coverslip was separated into four 9-panel mega-images. Each panel (1,024 × 1,024) was acquired with a 10× objective, and then, the panels were stitched together (10% overlap) using Olympus FluoView 1000 imaging software. The total cell number and cell area for each panel were calculated using Image Pro Analyzer software (Media Cybernetics).

Cell lysis for Western blotting. Adherent cells were washed in PBS and then lysed in the culture plate in radioimmunoprecipitation assay buffer (25 mM Tris HCl, pH 7.6, 150 mM NaCl, 1% Nonidet P40, 1% sodium deoxycholate, 0.1% sodium dodecyl sulfate) containing 1 mM phenylmethylsulfonyl fluoride, 10 μg/ml of aprotinin, 10 μg/ml of leupeptin, 10 μg/ml of soybean trypsin inhibitor, 10 mM sodium orthovanadate, 5 mM sodium fluoride, and 2 mM sodium pyrophosphate. The protein concentration in the cell lysates was determined using a Pierce bicinchoninic acid protein assay kit (Thermo Scientific).

Mice. Animal experiments were conducted in accordance with the protocol approved by the Institutional Animal Care and Use Committee of the La Jolla Institute for Allergy and Immunology (no. AP140-NB4). RPTPα-KO mice were generated as previously described (26). C57BL/6 KRN mice were provided by Dr. Christophe Benoist (Harvard Medical School, Boston, MA) and were crossed with NOD mice (The Jackson Laboratory) to obtain arthritic offspring (K/BxN mice) whose serum was pooled for use in the K/BxN passive serum-transfer arthritis model (27). Congenic CD45.1 C57BL/6 mice were purchased from Taconic Biosciences.

K/BxN passive serum-transfer arthritis model. Arthritis was induced in 8-week-old male and female mice by intraperitoneal injection of 200 μl of pooled serum from K/BxN mice. Every 2 days, ankle thickness was measured using digital calipers (27).

Reciprocal bone marrow transplantation. Male recipient mice were lethally irradiated with 2 doses of 550 rads and administered bone marrow from male donor mice. WT congenic CD45.1 mice were administered bone marrow cells from WT or RPTPα-KO CD45.2 mice, and WT and RPTPα-KO mice were administered bone marrow cells from WT congenic CD45.1 mice. At 10–11 weeks postirradiation, K/BxN pooled serum was administered to induce arthritis. The percentage of engrafted cells in WT recipients reconstituted with KO bone marrow and in KO recipients reconstituted with WT bone marrow was >90%.

Assessment of inflammation with an intravital probe. The Xenolight Rediject Inflammation Probe (PerkinElmer) is an intravital luminescent dye that penetrates phagocytic cells and enables visualization of joint infiltration. Seven days after arthritis induction, the probe was administered to mice by intraperitoneal injection according to the manufacturer's instructions. Joint inflammation was quantified using a Xenogen IVIS Spectrum in vivo imaging system (PerkinElmer).

Histologic analysis of arthritic joints. Hind paws were fixed in 10% neutral buffered formalin, decalcified, and embedded in paraffin. Sections were prepared from the tissue blocks and stained with hematoxylin and eosin and Safranin O–fast green–hematoxylin (HistoTox). Histopathologic scoring was performed as previously described (28). For bone erosion, joints were scored on a scale of 0–4, where 0 = normal, 1 = minimal (small areas of erosion, not readily apparent at low magnification), 2 = mild (more numerous areas of erosion, not readily apparent at low magnification, in trabecular or cortical bone), 3 = moderate (obvious erosion of trabecular and cortical bone, without full-thickness cortex defects; loss of some trabeculae;

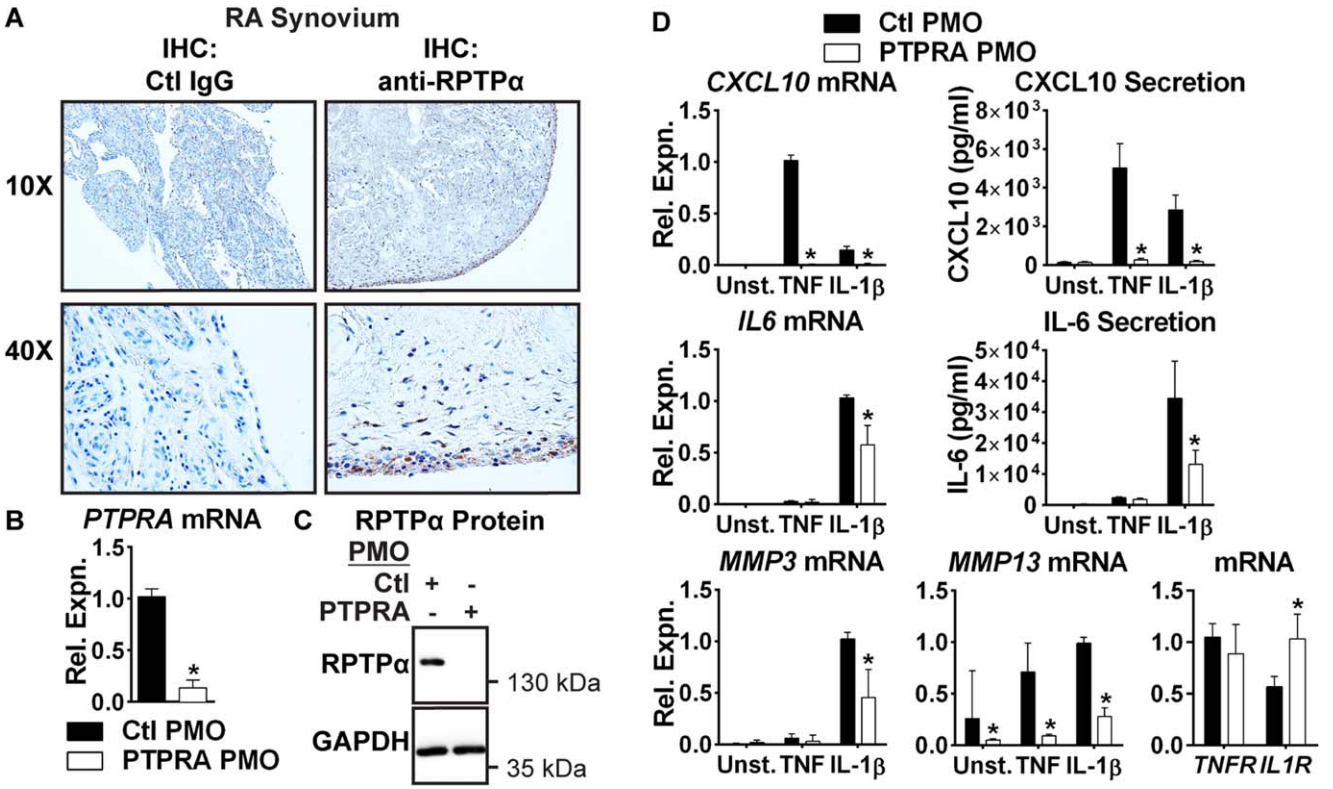

Figure 1. Receptor protein tyrosine phosphatase α (RPTPα) enrichment in the rheumatoid arthritis (RA) synovial lining and its promotion of tumor necrosis factor (TNF) and interleukin-1β (IL-1β) signaling in RA fibroblast-like synoviocytes (FLS). **A,** Immunohistochemical (IHC) analysis of RA synovial sections using anti-RPTPα or control IgG antibodies. **B,** Relative (Rel.) expression (Expn.) of mRNA for *PTPRA*, as determined by quantitative polymerase chain reaction (qPCR). RA FLS (n = 4) were treated for 7 days with 2.5 μM control nontargeting cell-permeable antisense oligonucleotide (PMO) or *PTPRA* PMO. Values are the median and interquartile range (IQR). $* = P < 0.05$ by Mann-Whitney test. **C,** RPTPα protein levels, as measured by Western blotting. **D,** Expression of mRNA for *CXCL10*, *IL6*, *MMP3*, and *MMP13*, as determined by qPCR, as well as protein levels of CXCL10 and IL-6, as determined by enzyme-linked immunosorbent assay. Following treatment with PMO, RA FLS (n = 4) were left unstimulated (Unst.) or were stimulated for 24 hours with 50 ng/ml of TNF or with 2 ng/ml of IL-1β. Values are the median and IQR. $* = P < 0.05$ versus control PMO–treated cells, by Mann-Whitney test.

lesions apparent at low magnification), and 4 = marked (full-thickness defects in the cortical bone and marked trabecular bone loss). Cartilage depletion was identified by diminished Safranin O staining of the matrix; staining was scored on a scale of 0–4, where 0 = no cartilage destruction (full Safranin O staining), 1 = localized cartilage erosions, 2 = more extended cartilage erosions, 3 = severe cartilage erosions, and 4 = depletion of the entire cartilage. Histologic analyses were performed in a blinded manner by 2 independent operators.

Joint extravasation assay. Mice were injected retroorbitally with AngioSense 680 probe according to the manufacturer's instructions (PerkinElmer), and after 5 minutes, they were injected intraperitoneally with arthritogenic K/BxN sera. After 1 hour, joint fluorescence was quantified using a Xenogen IVIS Spectrum imaging system.

Statistical analysis. The two-way analysis of variance, Mann-Whitney U test, Wilcoxon's matched pairs signed rank test, and chi-square test for independence were performed using GraphPad Prism software. *P* values less than 0.05 were considered significant.

RESULTS

RPTPα expression in fibroblasts from RA synovium. We first explored a possible role for RPTPα in RA FLS. We previously reported high levels of expression of the *PTPRA* gene in cultured RA FLS (11). In the present study, IHC analysis of human RA synovial sections revealed prominent RPTPα expression in the synovial intimal lining (Figure 1A). We examined whether *PTPRA* expression in RA FLS is affected by cell stimulation with inflammatory cytokines and found that stimulation of RA FLS with TNF and IL-1β had no effect on *PTPRA* expression (data not shown).

Promotion of the responsiveness of FLS to inflammatory cytokine stimulation by RPTPα. We next tested the effect of RPTPα deficiency on the response of RA FLS to TNF and IL-1β stimulation. We subjected

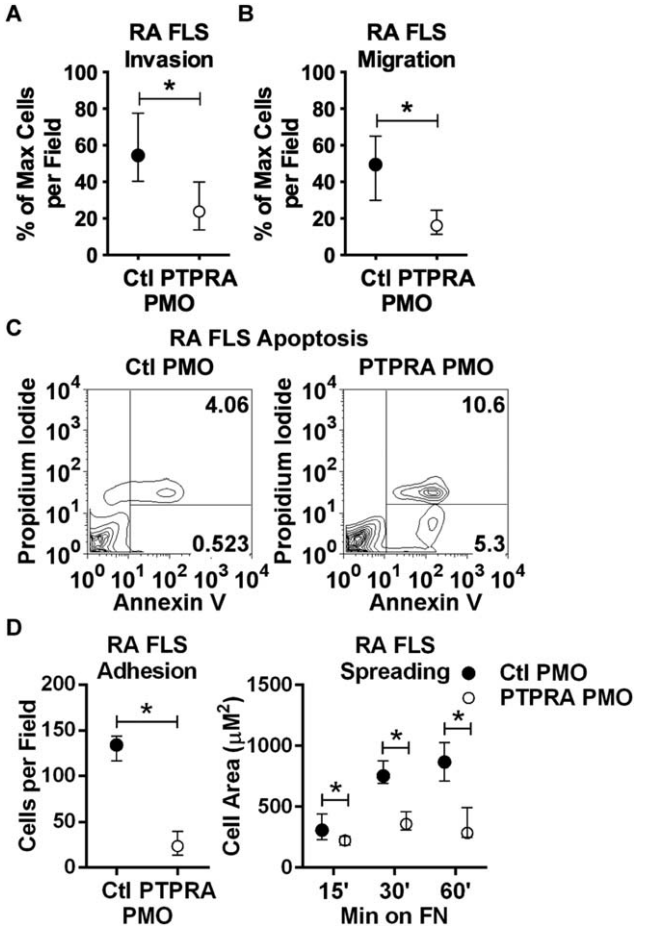

Figure 2. Promotion of RA FLS invasiveness by RPTPα. Cells were treated for 7 days with *PTPRA* or control PMO prior to analysis. **A,** Invasion of RA FLS (n = 4) through Matrigel-coated Transwell chambers for 48 hours in response to 50 ng/ml of platelet-derived growth factor type BB (PDGF-BB). **B,** Migration of RA FLS (n = 4) through uncoated Transwell chambers for 24 hours in response to 5% fetal bovine serum (FBS). Values in **A** and **B** are the median and IQR percentage of the maximum number of cells per field. $* = P < 0.05$ by Mann-Whitney test. **C,** Fluorescence analysis of RA FLS stimulated for 24 hours with 50 ng/ml of PDGF and then stained with annexin V and propidium iodide (PI), as determined by fluorescence-activated cell sorting, with gating to detect early apoptotic (annexin V+/PI–) and necrotic/late apoptotic (annexin V+/PI+) cells. Results are representative of 4 independent experiments. $\chi^2(2df) = 2{,}294$, $P < 0.0001$ for *PTPRA* PMO versus control PMO. **D,** Adhesion and spreading of RA FLS (n = 4). Cells were plated on fibronectin (FN)–coated coverslips in the presence of 5% FBS and the number of cells per field and the total cell area were determined after the indicated times. Values are the median and IQR. $* = P < 0.05$ by Wilcoxon's matched pairs signed rank test. See Figure 1 for other definitions.

RA FLS to RPTPα knockdown with cell-permeable antisense oligonucleotide (Figures 1B and C). Treatment with *PTPRA* PMO significantly reduced RA FLS production of *CXCL10* and *MMP13* in response to TNF and significantly reduced RA FLS production of *IL6*, *CXCL10*, *MMP3*, and *MMP13* in response to IL-1β (Figure 1D). We assessed whether these effects were due to down-regulation of TNF receptor (*TNFRSF1A*) or IL-1β receptor (*IL1R*) expression. We found no effect on the expression of *TNFRSF1A*; however, *PTPRA* PMO increased the expression of *IL1R* (Figure 1D). The effect on *CXCL10* and *IL6* was further confirmed by treatment of RA FLS with a second *PTPRA*-targeted PMO of a different sequence (data not shown). Taken together, these data suggest that RPTPα promotes the production of proinflammatory and proinvasive mediators by RA FLS in response to inflammatory cytokines. While a role for RPTPα in the regulation of IL-1β signaling has been previously reported (29–31), this is, to the best of our knowledge, the first report of a role of RPTPα in TNF signaling.

Promotion of RA FLS invasiveness by RPTPα. We next examined whether RPTPα affects the invasiveness of RA FLS. RA FLS invasiveness ex vivo has been shown to correlate with radiographic damage during RA progression (25). We subjected PMO-treated RA FLS to Transwell invasion assays through Matrigel in response to PDGF, a highly expressed promoter of FLS invasiveness in the RA synovium (4). RA FLS treated with *PTPRA* PMO, as compared to control nontargeting PMO–treated cells, were significantly less invasive in response to PDGF, with a median percentage of maximum cells per field of 54.4% (interquartile range [IQR] 40.3–77.5) after treatment with control PMO and 23.8% (IQR 13.7–40.0) after treatment with *PTPRA* PMO ($P < 0.05$) (Figure 2A).

We next assessed whether the effect of *PTPRA* PMO on RA FLS invasiveness was due to impaired cell motility. *PTPRA* PMO–treated cells showed significantly reduced migration in a Transwell assay in response to 5% FBS, with a median percentage of maximum cells per field of 49.4% (IQR 29.8–64.9) after treatment with control PMO and 16.1% (IQR 11.4–24.5 after treatment with *PTPRA* PMO) (Figure 2B). We hypothesized that this could be due to increased cell death or to reduced cytoskeletal reorganization following RPTPα knockdown. We therefore examined the effect of *PTPRA* PMO on cell apoptosis and necrosis and on cell spreading. RA FLS treated with *PTPRA* PMO showed significantly increased apoptosis as compared to control PMO–treated cells in serum-starvation medium (data not shown) or in the presence of PDGF (Figure 2C). We also found that live *PTPRA* PMO–treated cells were less adherent to, and displayed impaired spreading on, fibronectin-coated coverslips (Figure 2D). Taken together, these data strongly support a role of RPTPα in promoting RA FLS survival and growth factor–dependent cytoskeletal reorganization, migration, and invasiveness.

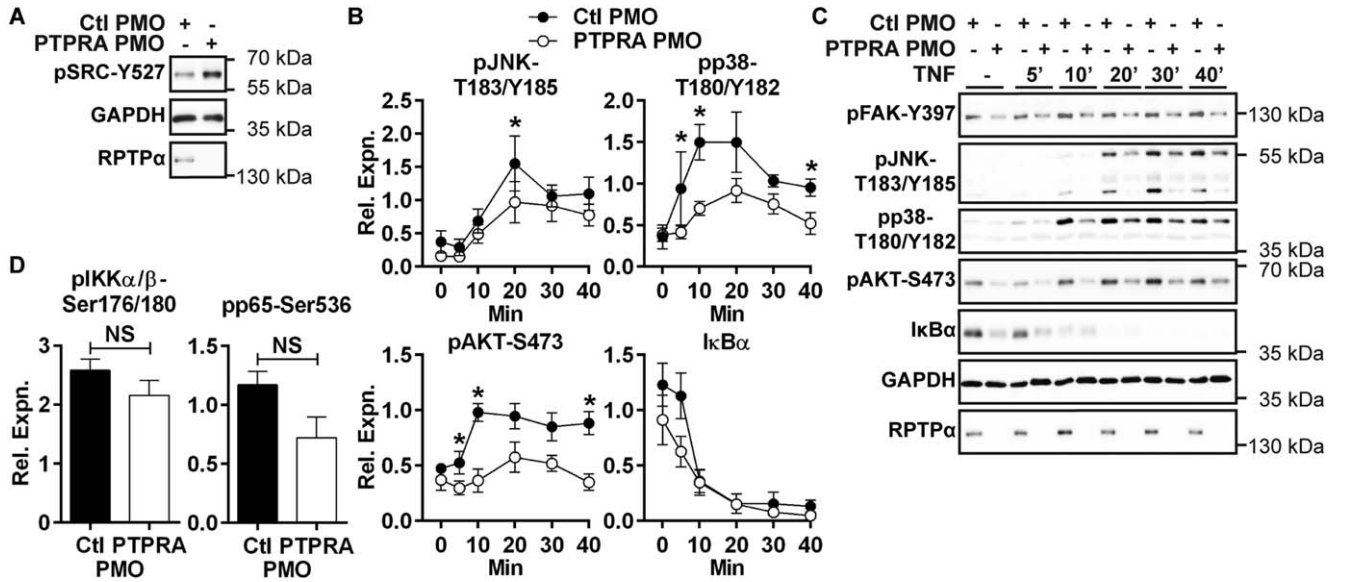

Figure 3. RPTPα-mediated promotion of RA FLS signaling downstream of Src. **A,** Anti–pSrc-Y^{527} levels in PMO-treated RA FLS lysates, as determined by Western blotting. Results are representative of 4 independent experiments. **B** and **C,** Western blotting of lysates of PMO-treated RA FLS that were left unstimulated or were stimulated with 50 ng/ml TNF for the indicated times. Signal intensities of Western blots of TNF-activated phosphorylated JNK-T^{183}/Y^{185}, p38-T^{180}/Y^{182}, Akt-S^{473}, and IκBα in cell lysates relative to GAPDH were quantified by densitometric scanning (**B**). Values are the mean ± SEM of 6 cell lines. $* = P < 0.05$ versus *PTPRA* PMO–treated cells, by Wilcoxon's matched pairs signed rank test. Western blots of the indicated TNF-activated phosphorylated kinases are representative of 4 independent experiments (**C**). **D,** Signal intensities of Western blots of lysates from unstimulated PMO-treated RA FLS for phosphorylated IKKα/β on Ser$^{176/180}$ and p65 on Ser^{536} relative to GAPDH. Values are the mean ± SEM of 6 cell lines. FAK = focal adhesion kinase; NS = not significant (see Figure 1 for other definitions).

RPTPα-mediated promotion of RA FLS aggressiveness through control of Src and FAK activation. The inhibitory Src tyrosine residue (Y^{527}) has been identified as the physiologic substrate of RPTPα in multiple cell types (14,16). Dephosphorylation of Src-Y^{527} enhances Src activation, leading to tyrosine phosphorylation of FAK-Y^{397} (a sub-

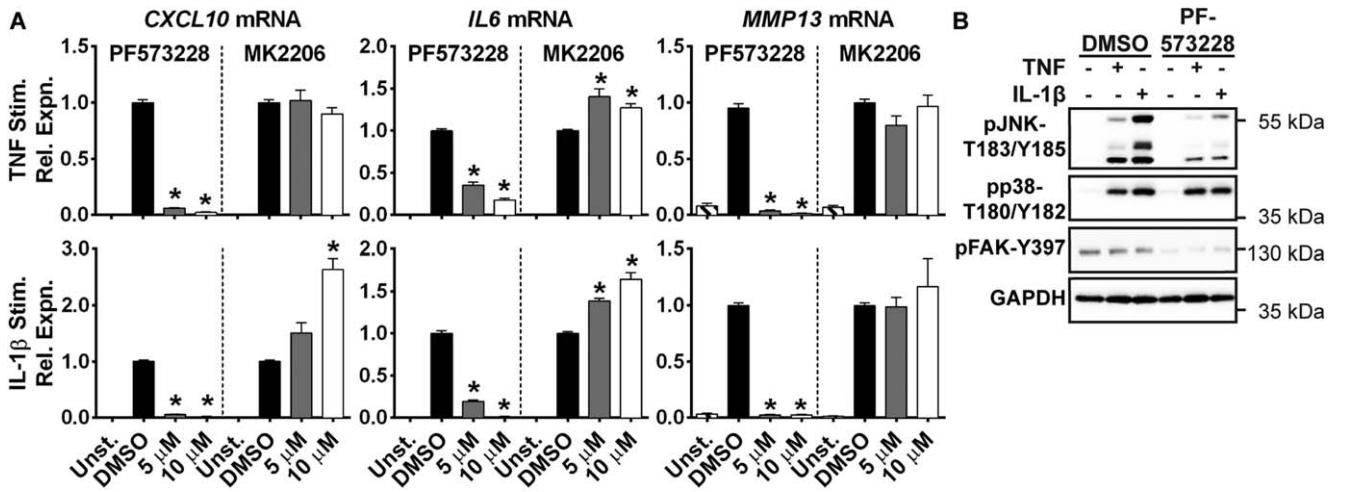

Figure 4. Impaired TNF- and IL-1β–induced gene expression and activation of JNK by focal adhesion kinase (FAK) inhibition in RA FLS. **A,** Expression of mRNA for *CXCL10*, *IL6*, and *MMP13* in RA FLS stimulated for 24 hours with TNF (50 ng/ml) or IL-1β (2 ng/ml) in the presence or absence of DMSO or the indicated concentrations of the FAK inhibitor PF573228 or the Akt inhibitor MK2206, as determined by qPCR. Values are the mean ± SEM of 4 cell lines. $* = P < 0.05$ versus DMSO-treated cells, by Mann-Whitney test. **B,** Western blots of RA FLS for phosphorylated JNK-T^{183}/Y^{185}, p38-T^{180}/Y^{182}, and FAK-Y^{397} in cell lysates relative to GAPDH. Cells were stimulated for 30 minutes with TNF (50 ng/ml) or IL-1β (2 ng/ml) in the presence or absence of DMSO or the FAK inhibitor PF573228. Results are representative of 4 independent experiments. See Figure 1 for other definitions.

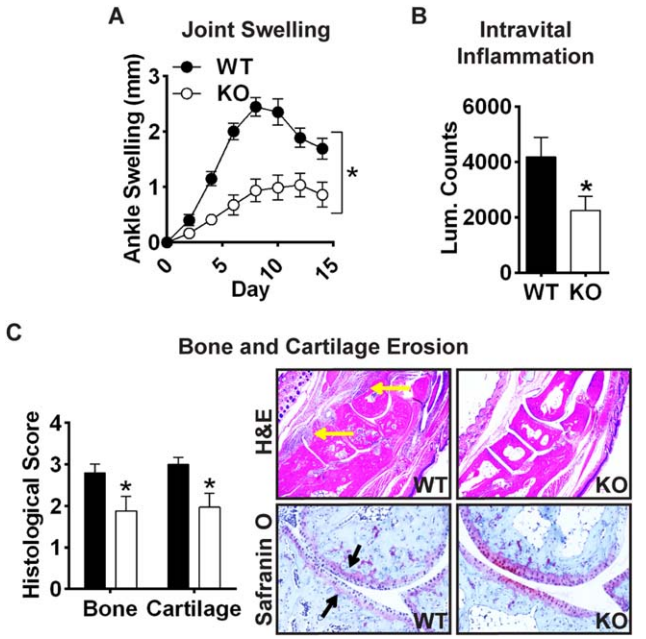

Figure 5. Resistance of RPTPα-knockout (KO) mice to K/BxN serum–transfer arthritis. Wild-type (WT) and RPTPα-KO littermate mice were administered 200 μl of K/BxN serum at 8 weeks of age. **A,** Ankle thickness was measured every 2 days. Values are the mean ± SEM of 16 WT and 17 KO mice. $* = P < 0.05$ by two-way analysis of variance. **B,** Luminescence of wrist and ankle joints was measured 7 days following serum transfer in mice injected with an intravital inflammation probe. Values are the mean ± SEM luminescence (Lum.) counts per joint in 3 mice per group. $* = P < 0.05$ by Wilcoxon's matched pairs signed rank test. **C,** Histologic analysis of ankles stained with hematoxylin and eosin (H&E) or Safranin O was performed at the end of the disease course. Histologic scores of bone and cartilage erosions are shown at the left. Values are the mean ± SEM of 16 WT and 17 KO mice. $* = P < 0.05$ by Wilcoxon's matched pairs signed rank test. Representative images of H&E-stained and Safranin O–stained joint sections are shown at the right. **Yellow arrows** indicate regions of inflammatory infiltrate. **Black arrows** indicate regions of cartilage erosion. Original magnification × 10.

strate of Src [7]) and other Src substrates. In RA FLS, phospho–Src-Y^{527} was found to be constitutive and not induced by TNF or IL-1β stimulation (data not shown). We hypothesized that RPTPα dephosphorylates phospho–Src-Y^{527} in RA FLS, so we assessed whether RPTPα knockdown in RA FLS influences basal Src-Y^{527} phosphorylation levels. We found that RPTPα knockdown increased the phosphorylation of Src-Y^{527} in resting RA FLS (Figure 3A).

Next, we assessed whether RPTPα knockdown affected signaling downstream of Src in RA FLS. We found that FAK-Y^{397} was constitutively phosphorylated in RA FLS. Phospho–FAK-Y^{397} was unaffected by TNF and IL-1β stimulation, and its phosphorylation was reduced by RPTPα knockdown (Figure 3C). As FAK promotes the activation of MAPKs (7) and is critical for JNK activation in RA FLS (32), we examined whether RPTPα knockdown affected TNF- and IL-1β–induced activation of the JNK and p38 MAPKs. We found that RPTPα knockdown impaired TNF- and IL-1β–stimulated phosphorylation of the activation motif of JNK-T^{183}/Y^{185} as well as p38-T^{180}/Y^{182} (Figures 3B and C and data not shown).

We also examined whether RPTPα promoted activation of the Akt and NF-κB signaling pathways, which are activated by inflammatory cytokine stimulation in RA FLS (4). As shown in Figures 3B and C, *PTPRA* PMO treatment reduced TNF- and IL-1β–stimulated phosphorylation of Akt-S^{473}. Interestingly, *PTPRA* PMO treatment caused a modest decrease in the levels of IκBα protein in resting RA FLS. Stimulation of cells with TNF or IL-1β, however, caused degradation of IκBα protein in both control and *PTPRA* PMO–treated cells, and by 10 minutes poststimulation, the levels of IκBα were similar between control and *PTPRA* PMO–treated cells (Figures 3B and C and data not shown). The trend toward decreased basal levels of IκBα in *PTPRA* PMO–treated cells was not accompanied by increased basal activation of the NF-κB pathway, but rather, we found a nonsignificant trend toward decreased basal phosphorylation of IKKα/β on Ser^{176}/Ser^{180} and NF-κB subunit p65 on Ser^{536} (Figure 3D). Additionally, we found that proteolytic processing of NF-κB subunits p100 and p105, as assessed by the ratio of p52 to p100 or p50 to p105, respectively, under basal conditions was unaffected by *PTPRA* knockdown (data not shown).

Pharmacologic inhibitors were then used to test whether FAK and Akt play essential roles in RA FLS induction of gene expression in response to TNF and IL-1β. Similar to the effect of RPTPα knockdown (Figure 1D), treatment of RA FLS with the FAK inhibitor PF573228 led to significantly decreased TNF- and IL-1β–induced production of *CXCL10*, *IL6*, and *MMP13* (Figure 4A). In contrast, treatment with the Akt inhibitor MK2206 did not dampen the expression of any these genes, but rather, it increased the expression of *IL6* and IL-1β–induced expression of *CXCL10* (Figure 4A).

The effects of the FAK inhibitor PF573228 on RA FLS signaling were further examined, and we confirmed that treatment of RA FLS with PF573228 does not cause the death of RA FLS at the concentrations used in these experiments (data not shown). We found that treatment of RA FLS with PF573228 impaired FAK-Y^{397} phosphorylation and TNF- and IL-1β–induced phosphorylation of JNK-T^{183}/Y^{185} (Figure 4B) but had no effect on p38-T^{180}/Y^{182} phosphorylation.

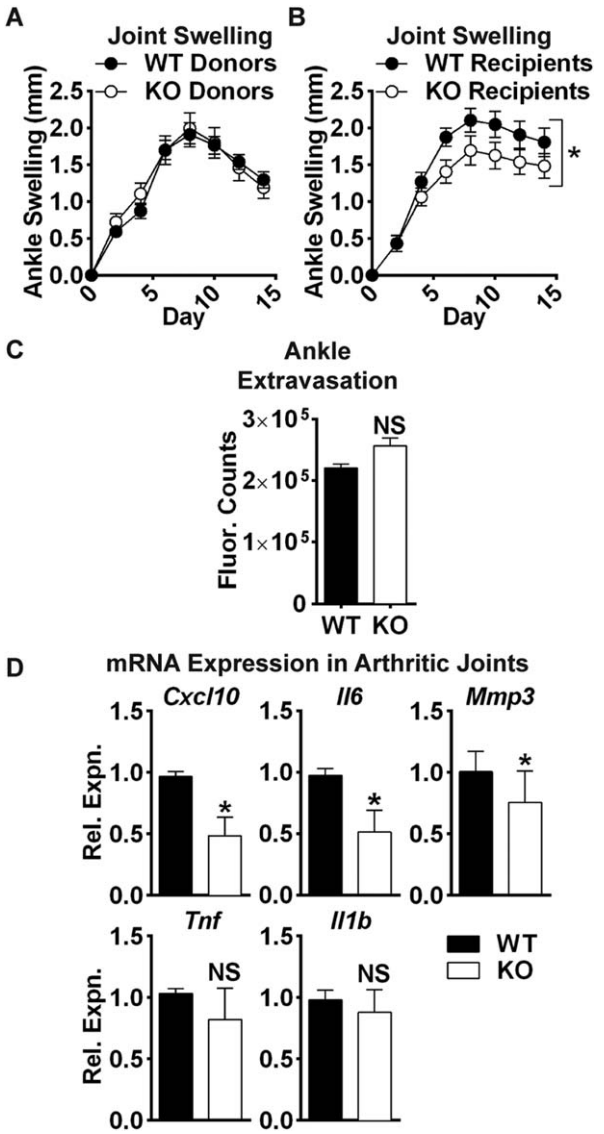

Figure 6. Dependence of arthritis protection upon radioresistant cells in RPTPα-knockout (KO) mice. **A** and **B,** Ankle thickness in donor and recipient mice was measured every 2 days. Mice were lethally irradiated and administered bone marrow from donor mice, and 10–11 weeks following irradiation, arthritis was induced in recipient mice by administration of K/BxN serum. Results are shown for male wild-type (WT) congenic CD45.1 mice administered bone marrow cells from WT (n = 19) or RPTPα-KO (n = 18) CD45.2 donor mice (**A**) and for male WT (n = 11) or RPTPα-KO (n = 11) mice administered bone marrow cells from WT congenic CD45.1 mice (**B**). Values are the mean ± SEM. * = $P < 0.05$ by two-way analysis of variance. **C,** Extravasation of fluorescent dye into the ankle joint was measured. WT (n = 5) and RPTPα-KO (n = 3) littermate mice were administered AngioSense 680 dye, followed by administration of K/BxN serum, and fluorescence in the ankle joint was determined after 60 minutes. Values are the median and interquartile range (IQR). **D,** Relative (Rel.) expression (Expn.) of mRNA for *Cxcl10*, *Il6*, *Mmp3*, *Tnf*, and *Il1b*. WT (n = 7) and RPTPα-KO (n = 7) mice were administered K/BxN serum, and after 8 days, the ankle joints were harvested and homogenized, and mRNA expression was analyzed by quantitative polymerase chain reaction. Values are the median and IQR. * = $P < 0.05$ by Mann-Whitney test. NS = not significant.

These findings strongly suggest that RPTPα promotes the TNF- and IL-1β–stimulated production of CXCL10, IL-6, and MMP-13 through a Src/FAK/JNK signaling pathway. RPTPα also likely promotes other signaling pathways in RA FLS, such as the Akt and p38 pathways, that are independent of FAK. Taken together, these data suggest a model whereby RPTPα mediates RA FLS aggressiveness by promoting the constitutive activation of Src and FAK, leading to enhanced FLS survival, increased production of critical mediators of arthritis in response to TNF and IL-1β, and promotion of motility and invasiveness in response to PDGF.

Resistance of RPTPα-KO mice to K/BxN passive-transfer arthritis through an effect on radioresistant cells. Having determined that RPTPα regulates the aggressive behavior of FLS ex vivo, we wanted to determine whether RPTPα mediates the pathogenic behavior of FLS in RA. We subjected WT and RPTPα-KO mice to the FLS-dependent K/BxN serum–transfer model of inflammatory arthritis and followed the disease course for 2 weeks. RPTPα-KO mice displayed significantly decreased arthritis severity, as assessed by measurements of ankle swelling (Figure 5A), joint inflammation (using an intravital probe) (Figure 5B), and bone and cartilage erosions (Figure 5C). RPTPα-KO does not cause a bone phenotype per se (33), suggesting that RPTPα promotes K/BxN serum–induced bone erosion through an effect on inflammation.

In the K/BxN serum–transfer model, disease development depends primarily upon the actions of innate immune cells and FLS (34–36). To determine whether disease protection in the RPTPα-KO mouse is due to recruited myeloid cells or radioresistant cells, such as FLS, we performed reciprocal bone marrow transplantation. WT recipient mice showed no difference in arthritis severity after transplantation with bone marrow from WT or RPTPα-KO donor mice (Figure 6A). However, RPTPα-KO recipient mice still showed significantly reduced severity of arthritis as compared to WT mice after transplantation with bone marrow from WT mice (Figure 6B). These data suggest that arthritis in this model is promoted by *Ptpra* through an effect on radioresistant cells.

To rule out effects of RPTPα on radioresistant cell types that control vascular permeability, we examined whether RPTPα-KO reduced acute K/BxN serum–induced extravasation to the ankles. We found no effect of RPTPα-KO using an intravital tracer (Figure 6C). Finally, upon examination of the expression of pathogenic mediators of disease in arthritic ankle homogenates, we found that RPTPα-KO mice exhibited significantly reduced expression of several genes produced by FLS during arthritis, including *Il6* and *Mmp3*, two important mediators of joint destruction in RA (4,37), as well as *Cxcl10*, a critical

pathogenic factor in mouse and human RA (38,39) (Figure 6D). RPTPα-KO mice also exhibited slightly reduced expression of *Tnf* and *Il1b*, inflammatory cytokines produced by immune cells that drive disease in the K/BxN model (Figure 6D). This is likely to be a secondary phenomenon due to decreased inflammatory infiltrate in the RPTPα-KO joint.

DISCUSSION

We report herein the first characterization of the role of RPTPα in FLS and in RA. RPTPα is expressed in the primary rheumatoid synovium and in cultured FLS. Knockdown of RPTPα expression impaired RA FLS induction of proinflammatory and proinvasive factors in response to TNF or IL-1β stimulation. Additionally, RPTPα knockdown reduced RA FLS invasiveness in response to PDGF, which is attributed to a combination of decreased survival, cytoskeletal reorganization, and motility. Our assessment of whether RPTPα mediates arthritis severity in the K/BxN mouse model, where FLS are critical to disease development (35), showed that *Ptpra* inactivation significantly reduced arthritis development. Reciprocal bone marrow transplantation revealed this to be due to radioresistant cells.

The decreased invasiveness, motility, and survival of RA FLS subjected to RPTPα knockdown is consistent with previous reports on the regulation of the Src/FAK pathway by RPTPα in other fibroblasts (14,16). Consistent with these reports, we observed that in resting RA FLS, loss of RPTPα increased the phosphorylation of Src-Y^{527} and impaired the phosphorylation of FAK-Y^{397}. Our investigation of the RPTPα-regulated pathways downstream of TNF and IL-1β showed that RPTPα knockdown reduced JNK, p38, and Akt phosphorylation after TNF and IL-1β stimulation. Through the use of chemical inhibitors, we identified the FAK/JNK pathway as being responsible for the effect of RPTPα on the expression of *CXCL10*, *IL6*, and *MMP13* after TNF and IL-1β stimulation. The observed increase in *IL6* expression after RA FLS treatment with the Akt inhibitor is interesting, given that this compound has been shown to attenuate RA FLS migration and invasiveness (40). The effect on IL-6 suggests that the Akt pathway can have differential effects on FLS aggressive phenotypes. The effect of RPTPα on Akt and p38 signaling warrants further future investigation.

The findings of our experiments strongly suggest that FLS at least partly mediate the reduced arthritis severity in RPTPα-KO mice. We can reasonably rule out the possibility that RPTPα promotes inflammation mediated by neutrophils, macrophages, or platelets, 3 radiosensitive cell types that contribute to pathogenicity in the K/BxN model (41–43). An effect on endothelial cells also is unlikely, since in our experiments, RPTPα did not affect K/BxN serum–induced vascular permeability. Mast cells are relatively radioresistant and play a controversial role in the K/BxN model (44); however, RPTPα-KO mice displayed increased IgE-dependent anaphylaxis, suggesting that RPTP KO does not suppress mast cell function (45). Since disease pathogenesis in the passive K/BxN model is lymphocyte-independent (36), this model has not allowed us to examine whether RPTPα plays a role in lymphocyte-mediated RA pathogenesis. However, peripheral T cell activation and proliferation were shown to be unaffected by RPTP KO (46). Since phospho-Src-Y^{527} is also targeted by the highly expressed PTP CD45, which is present only in hematopoietic cells, it is likely that redundancy between RPTPα and CD45 renders RPTPα less critical in adaptive immune cell signaling. Indeed, CD45 was reported to display much higher activity than RPTPα in T cells (47).

It was recently reported that *Fak* inactivation reduced FLS migration and invasiveness; however, global knockout of *Fak* did not affect disease severity in a TNF-induced mouse model of arthritis (48). A possible explanation for the difference in arthritis phenotypes between RPTPα-KO and FAK-KO mice could be that inactivation of *Fak* has opposing effects in FLS versus other arthritis-relevant cell types, such as immune cells. Thus, we speculate that RPTPα-KO mice do not phenocopy FAK-KO mice because RPTPα-KO affects FAK signaling only in nonimmunologic cell types.

The findings of this study suggest that inhibiting RPTPα may be therapeutically beneficial in RA. The recent report that RPTPα-KO mice are protected from fibrosis in a systemic sclerosis model (20) indicates that RPTPα could be an attractive target for combating other autoimmune diseases. Since these studies involved global *Ptpra* inactivation from the embryonic stage, determining whether acute deletion or pharmacologic inhibition of *Ptpra* in adult mice reverses established disease will be helpful in assessing whether RPTPα holds value as a therapeutic target. Additionally, since RPTPα promotes growth of transformed cells, it is also considered a potential drug target for cancer (49,50). Taken together, these findings suggest that exploration of the therapeutic potential of RPTPα is warranted.

ACKNOWLEDGMENTS

The authors are grateful to the CTRI Biorepository at UCSD for the FLS lines, to Dr. Catherine Pallen for critical review of the data, to Dr. Karen Doody for histologic scoring of slides, and to Jay Sharma for data collection.

AUTHOR CONTRIBUTIONS

All authors were involved in drafting the article or revising it critically for important intellectual content, and all authors approved the final version to be published. Dr. Bottini had full access to all of the data in the study and takes responsibility for the integrity of the data and the accuracy of the data analysis.

Study conception and design. Stanford, Sacchetti, Pilo, Wu, Kiosses, Corr, Firestein, Bottini.

Acquisition of data. Stanford, Svensson, Sacchetti, Pilo, Wu, Kiosses, Hellvard, Bergum, Muench, Elly, Liu, Hertog, Elson, Sap, Mydel, Boyle.

Analysis and interpretation of data. Stanford, Svensson, Sacchetti, Pilo, Wu, Kiosses, Muench, Bottini.

REFERENCES

1. Ospelt C, Neidhart M, Gay RE, Gay S. Synovial activation in rheumatoid arthritis. Front Biosci 2004;9:2323–34.
2. Lefevre S, Knedla A, Tennie C, Kampmann A, Wunrau C, Dinser R, et al. Synovial fibroblasts spread rheumatoid arthritis to unaffected joints. Nat Med 2009;15:1414–20.
3. Neumann E, Lefevre S, Zimmermann B, Gay S, Muller-Ladner U. Rheumatoid arthritis progression mediated by activated synovial fibroblasts. Trends Mol Med 2010;16:458–68.
4. Bottini N, Firestein GS. Duality of fibroblast-like synoviocytes in RA: passive responders and imprinted aggressors. Nat Rev Rheumatol 2013;9:24–33.
5. Noss EH, Brenner MB. The role and therapeutic implications of fibroblast-like synoviocytes in inflammation and cartilage erosion in rheumatoid arthritis. Immunol Rev 2008;223:252–70.
6. Niedermeier M, Pap T, Korb A. Therapeutic opportunities in fibroblasts in inflammatory arthritis. Best Pract Res Clin Rheumatol 2010;24:527–40.
7. Mitra SK, Hanson DA, Schlaepfer DD. Focal adhesion kinase: in command and control of cell motility. Nat Rev Mol Cell Biol 2005;6: 56–68.
8. Hanks SK, Ryzhova L, Shin NY, Brabek J. Focal adhesion kinase signaling activities and their implications in the control of cell survival and motility. Front Biosci 2003;8:d982–96.
9. Shahrara S, Castro-Rueda HP, Haines GK, Koch AE. Differential expression of the FAK family kinases in rheumatoid arthritis and osteoarthritis synovial tissues. Arthritis Res Ther 2007;9:R112.
10. Nakano K, Whitaker JW, Boyle DL, Wang W, Firestein GS. DNA methylome signature in rheumatoid arthritis. Ann Rheum Dis 2013;72:110–7.
11. Stanford SM, Maestre MF, Campbell AM, Bartok B, Kiosses WB, Boyle DL, et al. Protein tyrosine phosphatase expression profile of rheumatoid arthritis fibroblast-like synoviocytes: a novel role of SH2 domain–containing phosphatase 2 as a modulator of invasion and survival. Arthritis Rheum 2013;65:1171–80.
12. Zeng L, Si X, Yu WP, Le HT, Ng KP, Teng RM, et al. PTP α regulates integrin-stimulated FAK autophosphorylation and cytoskeletal rearrangement in cell spreading and migration. J Cell Biol 2003;160:137–46.
13. Cheng SY, Sun G, Schlaepfer DD, Pallen CJ. Grb2 promotes integrin-induced focal adhesion kinase (FAK) autophosphorylation and directs the phosphorylation of protein tyrosine phosphatase α by the Src-FAK kinase complex. Mol Cell Biol 2014;34:348–61.
14. Su J, Muranjan M, Sap J. Receptor protein tyrosine phosphatase α activates Src-family kinases and controls integrin-mediated responses in fibroblasts. Curr Biol 1999;9:505–11.
15. Sap J, D'Eustachio P, Givol D, Schlessinger J. Cloning and expression of a widely expressed receptor tyrosine phosphatase. Proc Natl Acad Sci U S A 1990;87:6112–6.
16. Pallen CJ. Protein tyrosine phosphatase alpha (PTPα): a Src family kinase activator and mediator of multiple biological effects. Curr Top Med Chem 2003;3:821–35.
17. Zheng XM, Wang Y, Pallen CJ. Cell transformation and activation of pp60c-src by overexpression of a protein tyrosine phosphatase. Nature 1992;359:336–9.
18. Den Hertog J, Pals CE, Peppelenbosch MP, Tertoolen LG, de Laat SW, Kruijer W. Receptor protein tyrosine phosphatase α activates pp60c-src and is involved in neuronal differentiation. EMBO J 1993;12:3789–98.
19. Ponniah S, Wang DZ, Lim KL, Pallen CJ. Targeted disruption of the tyrosine phosphatase PTPα leads to constitutive downregulation of the kinases Src and Fyn. Curr Biol 1999;9:535–8.
20. Aschner Y, Khalifah AP, Briones N, Yamashita C, Dolgonos L, Young SK, et al. Protein tyrosine phosphatase α mediates profibrotic signaling in lung fibroblasts through TGF-β responsiveness. Am J Pathol 2014;184:1489–502.
21. Alvaro-Gracia JM, Zvaifler NJ, Brown CB, Kaushansky K, Firestein GS. Cytokines in chronic inflammatory arthritis. VI. Analysis of the synovial cells involved in granulocyte-macrophage colony-stimulating factor production and gene expression in rheumatoid arthritis and its regulation by IL-1 and tumor necrosis factor-α. J Immunol 1991;146: 3365–71.
22. Arnett FC, Edworthy SM, Bloch DA, McShane DJ, Fries JF, Cooper NS, et al. The American Rheumatism Association 1987 revised criteria for the classification of rheumatoid arthritis. Arthritis Rheum 1988;31:315–24.
23. Radonic A, Thulke S, Mackay IM, Landt O, Siegert W, Nitsche A. Guideline to reference gene selection for quantitative real-time PCR. Biochem Biophys Res Commun 2004;313:856–62.
24. Laragione T, Brenner M, Mello A, Symons M, Gulko PS. The arthritis severity locus Cia5d is a novel genetic regulator of the invasive properties of synovial fibroblasts. Arthritis Rheum 2008; 58:2296–306.
25. Tolboom TC, van der Helm-Van Mil AH, Nelissen RG, Breedveld FC, Toes RE, Huizinga TW. Invasiveness of fibroblast-like synoviocytes is an individual patient characteristic associated with the rate of joint destruction in patients with rheumatoid arthritis. Arthritis Rheum 2005;52:1999–2002.
26. Bodrikov V, Leshchyns'ka I, Sytnyk V, Overvoorde J, den Hertog J, Schachner M. RPTPα is essential for NCAM-mediated $p59^{fyn}$ activation and neurite elongation. J Cell Biol 2005;168:127–39.
27. Monach PA, Mathis D, Benoist C. The K/BxN arthritis model. Curr Protoc Immunol 2008;15:15.22.
28. Guma M, Ronacher L, Liu-Bryan R, Takai S, Karin M, Corr M. Caspase 1–independent activation of interleukin-1β in neutrophil-predominant inflammation. Arthritis Rheum 2009;60:3642–50.
29. Wang Q, Rajshankar D, Branch DR, Siminovitch KA, Herrera Abreu MT, Downey GP, et al. Protein-tyrosine phosphatase-α and Src functionally link focal adhesions to the endoplasmic reticulum to mediate interleukin-1-induced Ca2+ signaling. J Biol Chem 2009; 284:20763–72.
30. Wang Q, Rajshankar D, Laschinger C, Talior-Volodarsky I, Wang Y, Downey GP, et al. Importance of protein-tyrosine phosphatase-α catalytic domains for interactions with SHP-2 and interleukin-1-induced matrix metalloproteinase-3 expression. J Biol Chem 2010;285:22308–17.
31. Rajshankar D, Sima C, Wang Q, Goldberg SR, Kazembe M, Wang Y, et al. Role of PTPα in the destruction of periodontal connective tissues. PLoS One 2013;8:e70659.
32. Stanford SM, Aleman Muench GR, Bartok B, Sacchetti C, Kiosses WB, Sharma J, et al. TGFβ responsive tyrosine phosphatase promotes rheumatoid synovial fibroblast invasiveness. Ann Rheum Dis 2014. E-pub ahead of print.
33. Finkelshtein E, Lotinun S, Levy-Apter E, Arman E, den Hertog J, Baron R, et al. Protein tyrosine phosphatases ϵ and α perform nonredundant roles in osteoclasts. Mol Biol Cell 2014;25:1808–18.
34. Ji H, Ohmura K, Mahmood U, Lee DM, Hofhuis FM, Boackle SA, et al. Arthritis critically dependent on innate immune system players. Immunity 2002;16:157–68.
35. Lee DM, Kiener HP, Agarwal SK, Noss EH, Watts GF, Chisaka O, et al. Cadherin-11 in synovial lining formation and pathology in arthritis. Science 2007;315:1006–10.
36. Wang Y, Shaked I, Stanford SM, Zhou W, Curtsinger JM, Mikulski Z, et al. The autoimmunity-associated gene PTPN22 potentiates

Toll-like receptor-driven, type 1 interferon-dependent immunity. Immunity 2013;39:111–22.
37. Baumann H, Kushner I. Production of interleukin-6 by synovial fibroblasts in rheumatoid arthritis. Am J Pathol 1998;152:641–4.
38. Hanaoka R, Kasama T, Muramatsu M, Yajima N, Shiozawa F, Miwa Y, et al. A novel mechanism for the regulation of IFN-γ inducible protein-10 expression in rheumatoid arthritis. Arthritis Res Ther 2003;5:R74–81.
39. Lee EY, Lee ZH, Song YW. The interaction between CXCL10 and cytokines in chronic inflammatory arthritis. Autoimmun Rev 2013;12: 554–7.
40. Fan W, Zhou ZY, Huang XF, Bao CD, Du F. Deoxycytidine kinase promotes the migration and invasion of fibroblast-like synoviocytes from rheumatoid arthritis patients. Int J Clin Exp Pathol 2013;6:2733–44.
41. Wipke BT, Allen PM. Essential role of neutrophils in the initiation and progression of a murine model of rheumatoid arthritis. J Immunol 2001;167:1601–8.
42. Boilard E, Nigrovic PA, Larabee K, Watts GF, Coblyn JS, Weinblatt ME, et al. Platelets amplify inflammation in arthritis via collagen-dependent microparticle production. Science 2010;327:580–3.
43. Guma M, Hammaker D, Topolewski K, Corr M, Boyle DL, Karin M, et al. Antiinflammatory functions of p38 in mouse models of rheumatoid arthritis: advantages of targeting upstream kinases MKK-3 or MKK-6. Arthritis Rheum 2012;64:2887–95.
44. Nigrovic PA, Malbec O, Lu B, Markiewski MM, Kepley C, Gerard N, et al. C5a receptor enables participation of mast cells in immune complex arthritis independently of Fcγ receptor modulation. Arthritis Rheum 2010;62:3322–33.
45. Samayawardhena LA, Pallen CJ. PTPα activates Lyn and Fyn and suppresses Hck to negatively regulate FcεRI-dependent mast cell activation and allergic responses. J Immunol 2010;185: 5993–6002.
46. Maksumova L, Le HT, Muratkhodjaev F, Davidson D, Veillette A, Pallen CJ. Protein tyrosine phosphatase α regulates Fyn activity and Cbp/PAG phosphorylation in thymocyte lipid rafts. J Immunol 2005;175:7947–56.
47. Ng DH, Jabali MD, Maiti A, Borodchak P, Harder KW, Brocker T, et al. CD45 and RPTPα display different protein tyrosine phosphatase activities in T lymphocytes. Biochem J 1997;327:867–76.
48. Shelef MA, Bennin DA, Yasmin N, Warner TF, Ludwig T, Beggs HE, et al. Focal adhesion kinase is required for synovial fibroblast invasion, but not murine inflammatory arthritis. Arthritis Res Ther 2014;16:464.
49. Gil-Henn H, Elson A. Tyrosine phosphatase-ε activates Src and supports the transformed phenotype of Neu-induced mammary tumor cells. J Biol Chem 2003;278:15579–86.
50. Zheng X, Resnick RJ, Shalloway D. Apoptosis of estrogen-receptor negative breast cancer and colon cancer cell lines by PTPα and src RNAi. Int J Cancer 2008;122:1999–2007.